Roman Coronagraph Instrument Reference Information

July 2022

Roman Coronagraph Science and Engineering Project Teams
Jet Propulsion Laboratory, California Institute of Technology

© 2022 California Institute of Technology. Government sponsorship acknowledged. The research was carried out in part at the Jet Propulsion Laboratory, California Institute of Technology, under a contract with the National Aeronautics and Space Administration. This document has been reviewed and determined not to contain export controlled technical data.

Critical Technology Demonstrations

The Roman Coronagraph is an advanced technology demonstrator for future missions that will directly image Earth-like exoplanets.

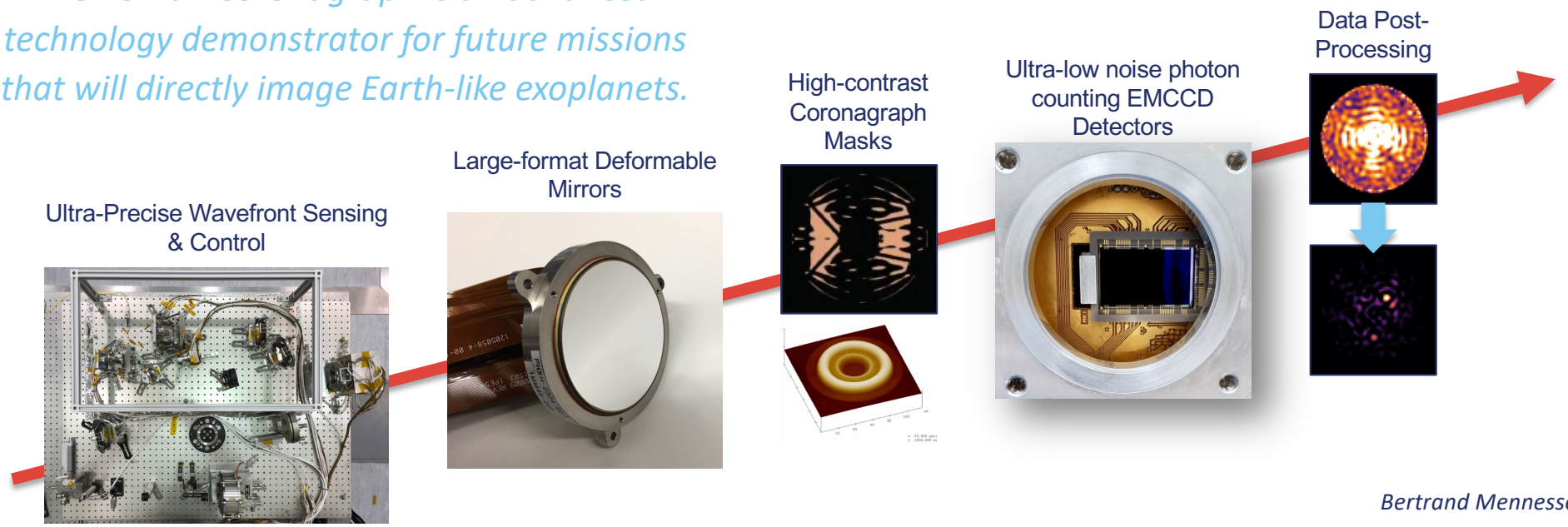

Bertrand Mennesson (JPL)

The Roman Coronagraph will premiere in space the technologies needed by future missions to image and characterize rocky planets in the habitable zones of nearby stars. By demonstrating these tools in a system with end-to-end, scientific observing operations, NASA will reduce the cost and risk of a potential future flagship mission.

Required & Predicted Coronagraph Performance in the Context of Existing Astronomy Capabilities

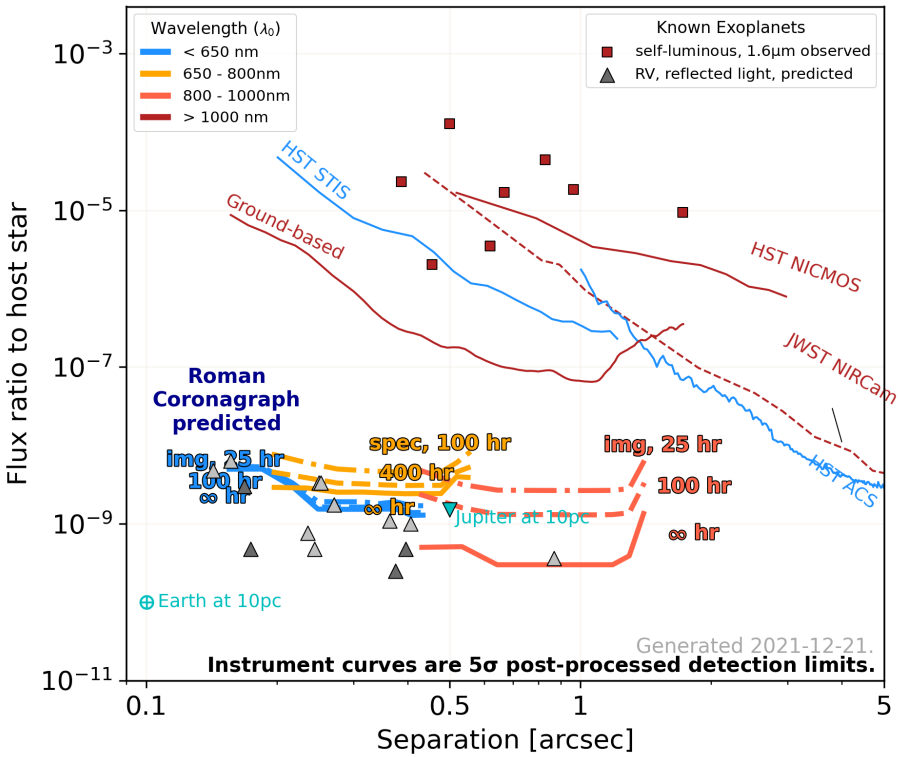

Instrument performance requirements and current-best-estimated performance are based on laboratory demonstrations and model predictions, as of December 21, 2021. Laboratory demonstrations and model refinements are ongoing.

See V. Bailey, https://github.com/nasavbailey/DI-flux-ratio-plot for a detailed description of this plot.

Coronagraph Community Participation Program

- Team that will use Roman's Coronagraph Instrument to meet its objectives associated with an in-space technology demonstration of a high-contrast coronagraph.
- Opportunity for proposers to work with the coronagraph instrument team to plan and execute its technology demonstration observations.
- Proposals accepted only from small groups. PI of each selected investigation, plus coronagraph project & international partner representatives, form the Community Participation Program Team.
- Certain focus areas will be identified in the solicitation (things like target/observation prep work; simulations; operation preparation; data analysis tools). Proposers can choose from the list, and can include other areas.

Potential Technology Demonstration Phase Observations

- Self luminous planet image and spectra
- Reflected light planet image and spectrum
- Bright debris disk polarimetry
- Faint debris disk detection

Coronagraph Architecture

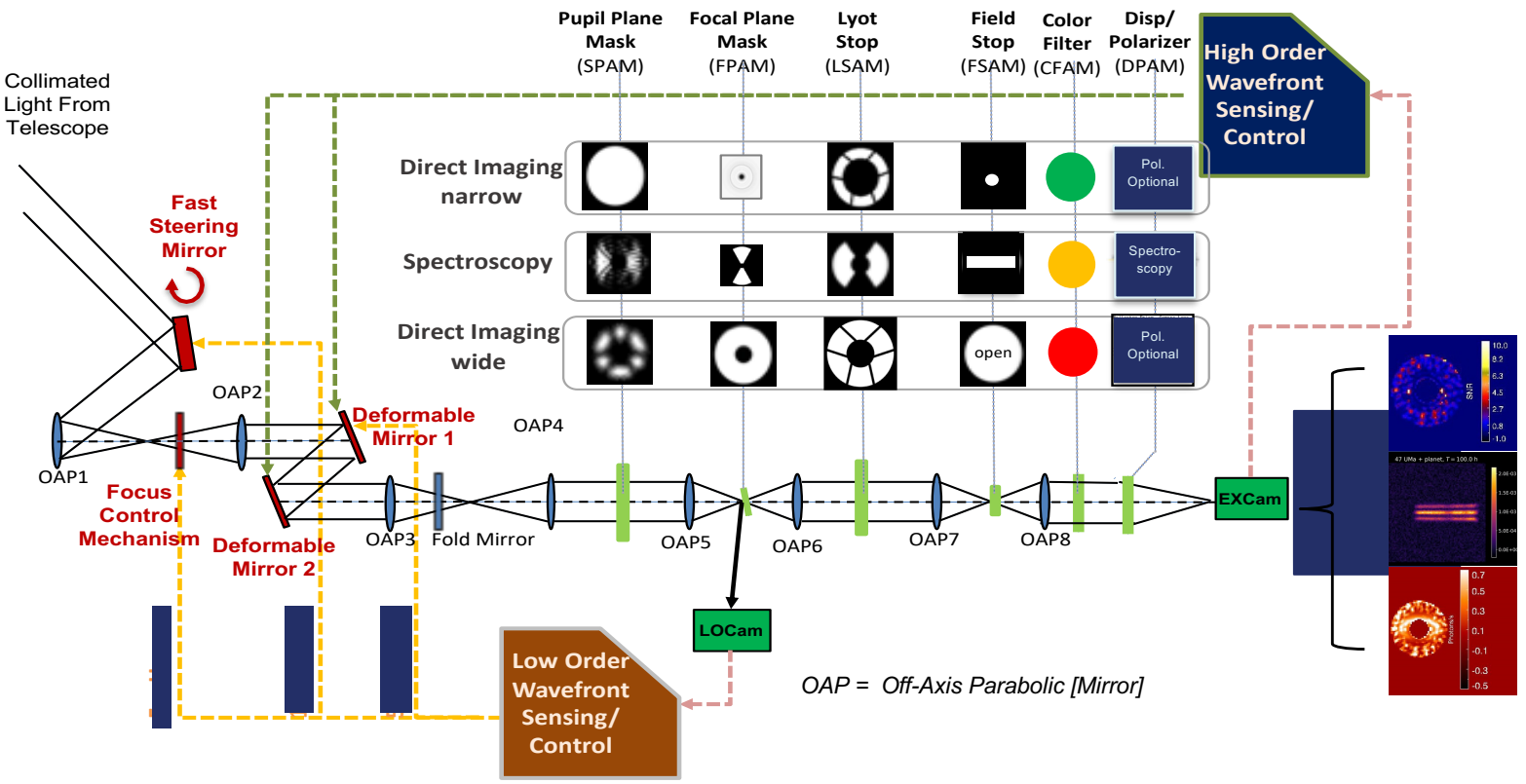

- Three observation modes implemented with three different sets of masks/filters
- Share the same optical beam train, with two wavefront control loops to achieve high contrast (better than 1E-8)

Coronagraph Architecture

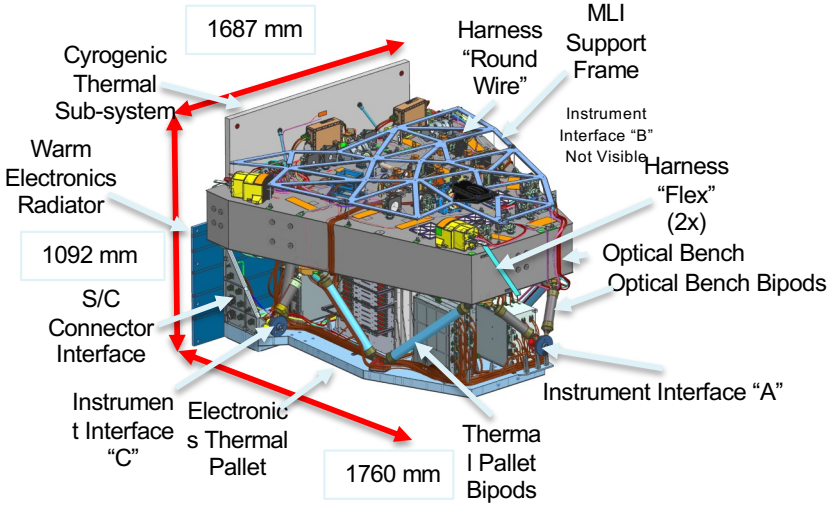

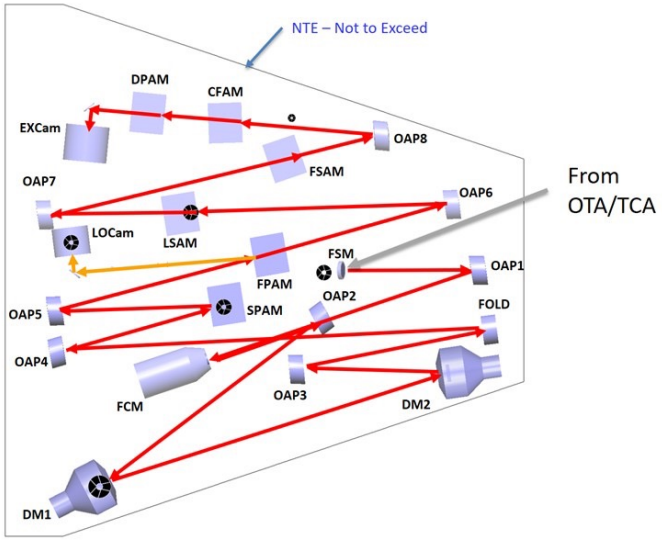

- In the Roman Payload, the Coronagraph Instrument mounts onto the Instrument Carrier (IC) shared with the Wide Field Instrument. The Tertiary Collimator Assembly (TCA; not shown) is the optical interface between the telescope and CGI, and relays an exit pupil onto the Fast Steering Mirror (FSM).
- Phase C design as of November 2020.

- The first deformable mirror, **DM 1**, is positioned at a relay pupil following the **FSM**. **DM 2** is positioned 1 meter away to enable correction of amplitude errors and phase errors originating from out-of-pupil surfaces.
- Both coronagraph mask types, the Hybrid Lyot and Shaped Pupil Coronagraphs (HLC and SPC), are implemented on the same optical beam train and selected by changing masks at the planes labeled **SPAM, FPAM, LSAM, and FSAM.**
- Observing mode is selected by mechanisms after the Lyot stop.

Coronagraph Elements

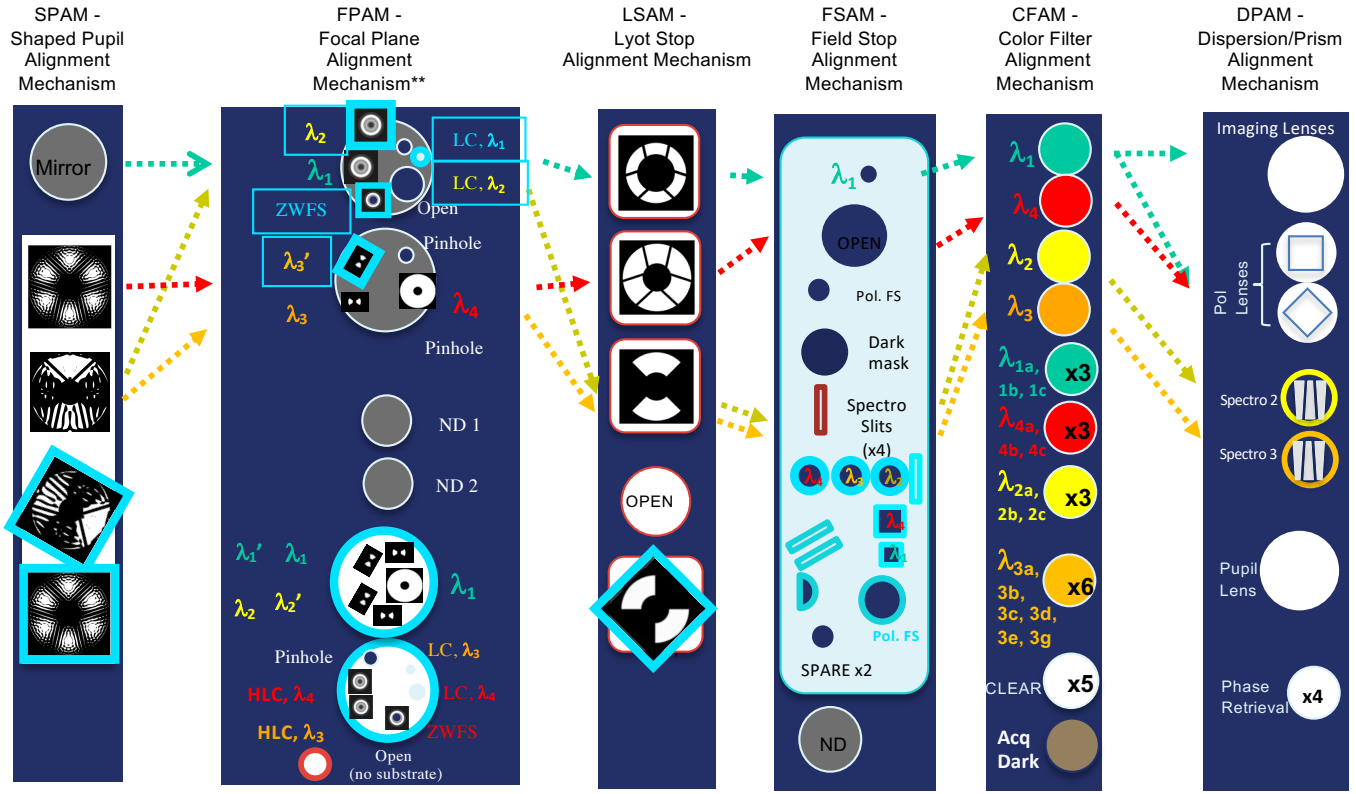

**Magnified for illustration. Each FPAM substrate can carry multiple coronagraphic elements.

Blue indicated contributed optics that are not part of requirements

λ_1 = 575 nm, 10% λ_2 = 660 nm, 15%
λ_3 = 730 nm, 15% λ_4 = 825 nm, 10%

Roman Coronagraph Passbands

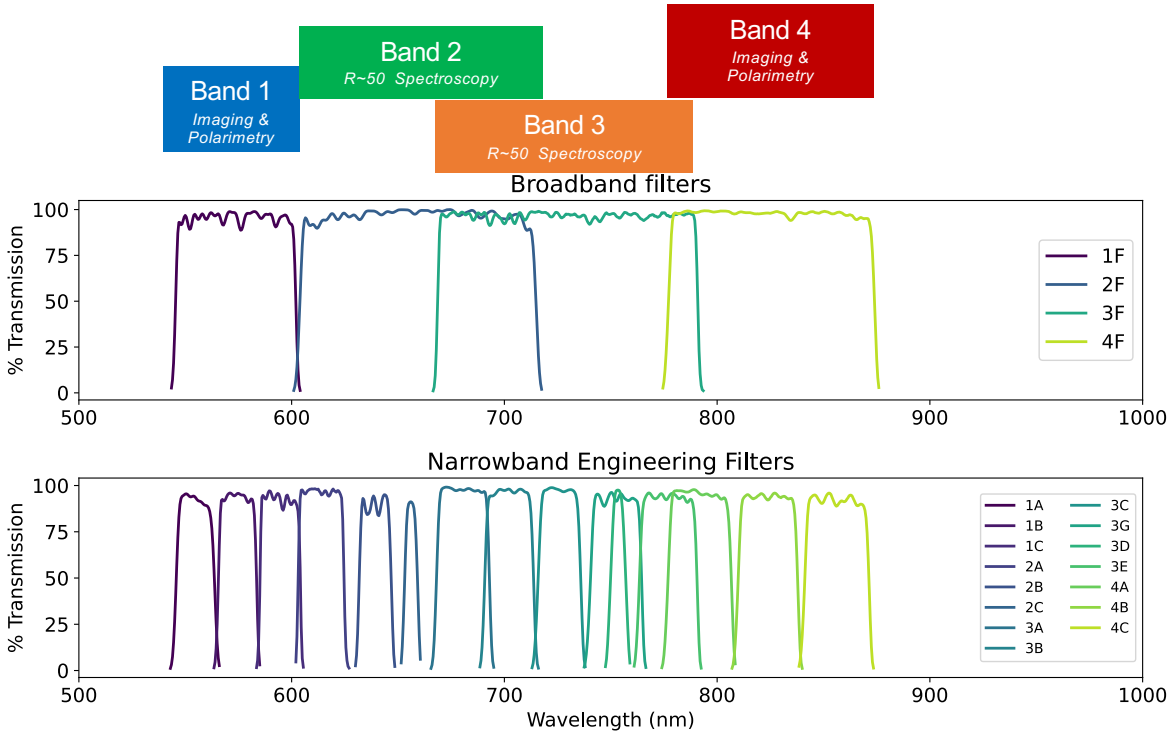

Three “official” modes will be fully tested prior to launch (Bands 1, 3, and 4)

Additional modes installed but not fully tested before launch

Observing Modes

Band	λ_{center}	FWHM	BW	Mode	FOV radius	FOV Coverage	Pol.	Coronagraph Mask Type	Support Status
1	573.8 nm	56.5 nm	9.8%	Narrow FOV Imaging	0.14” – 0.45”	360°	Y	Hybrid Lyot	Required (TTR5)
2	659.4 nm*	110.9 nm	16.8%	Slit + R~50 Prism Spectroscopy	0.17” – 0.52”	2 x 65°	-	Shaped Pupil	Unsupported
3	729.3 nm	122.3 nm	16.8%	Slit + R~50 Prism Spectroscopy	0.18” – 0.55”	2 x 65°	-	Shaped Pupil	Best effort
4	825.5 nm	96.8 nm	11.7%	“Wide” FOV Imaging	0.45” – 1.4”	360°	Y	Shaped Pupil	Best effort

All masks have been fabricated.

*** 660 nm spectroscopy** is the lowest priority for fabrication, implementation, and on-sky testing. If resources are limited, this mode may not be exercised during the Technology Demonstration Phase.

“Best effort” (Bands 2, 3, 4) modes will not be end-to-end performance tested prior to launch. They will be tested at component and assembly level (eg: are masks aligned in their mounting plates?). Prioritize hardware and fixed firmware over software that could be completed after CGI delivery. Most key hardware for the ‘best effort’ modes is in hand already. Software development is prioritizing Band 1 + HLC. It is possible that there will not be time to complete all software for one or more of the “best effort” modes prior to CGI delivery to payload integration and test, though nothing other than resources would preclude completing later.

Filters

name	λ_0 [nm]	FWHM [nm]	Primary Purpose
1F (1) *	573.8	56.5	Obs
2F (2)	659.4	110.9	Obs
3F (3)	729.3	122.3	Obs
4F (4)	825.5	96.8	Obs
1A	554.8	18	WFS **
1B	574.5	18	WFS
1C	594.7	19	WFS
2A	614.2	21.6	WFS
2B	639.4	15.1	WFS
2C	656	6.2	Wavecal ***
3A	680.6	24.9	WFS
3B	702.3	23	WFS
3C	725.9	20	WFS
3G	752.5	24.1	WFS
3D	753.3	7.2	Wavecal
3E	777.1	27.1	WFS
4A	791.7	29.8	WFS
4B	823.9	28	WFS
4C	856.5	30.2	WFS

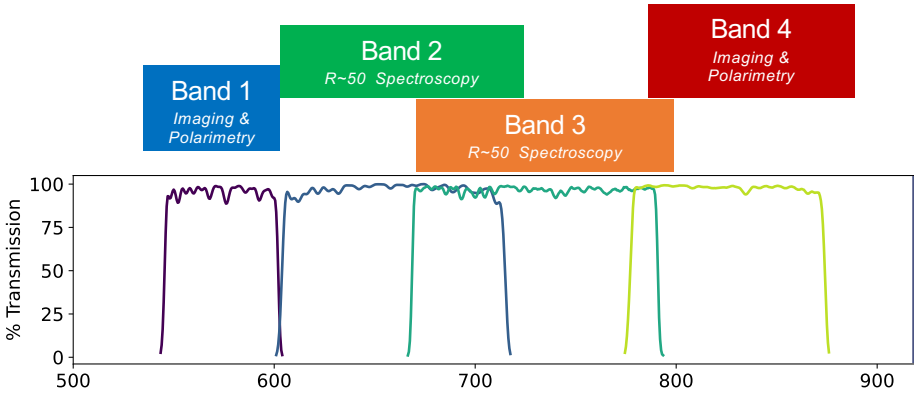

* Bands 1, 2, 3, 4 are shorthand for Bands 1F, 2F, 3F, 4F

** WFS = High-order wavefront sensing
*** Wavecal = spectroscopy wavelength calibration

https://roman.ipac.caltech.edu/sims/Param_db.html

Not all mask+filter combinations are valid

- High-Contrast masks are designed to operate at a specific wavelength (Band 1, 2, 3, or 4).
  - In principle, can be used with sub-bands of primary band (eg: SPC bowtie for Band 2 would also work for Band 2A, 2B, 2C, 3A, 3B, because they're all subsets of band 2).
- Combinations other than the supported ones (slide 10) may not be commissioned during the Tech Demo Phase

Unsupported observing modes

- Band 2 slit spectroscopy is now an unsupported observing mode
- Additional masks contributed by NASA's Exoplanet Exploration Program to fill empty slots in mechanisms.
  - Bands 2 and 3 spectroscopy with 60˚ rotated slit
  - Bands 1 and 4 Wide FOV with grid dot mask for multi-star WFC
  - Bands 2, 3, 4 HLC
  - "low contrast" classical Lyot stops with large inner working angles for "outside the dark hole" observations
  - Transmissive Zernike WFS dimples for focal plane WFS demo
- Caveat: No funding for on-sky commissioning identified at this time. Analogous to HST/STIS Bar5.
- For more info: see Riggs+ SPIE O&P 2021

Target constraints for coronagraphic observations

Reference Star
V < 3
<~ 1 mas angular diameter
Hot O/B
WFSC & PSF reference

Target Star
V < 5 (maybe V<7; TBD)
< 2 mas strongly preferred

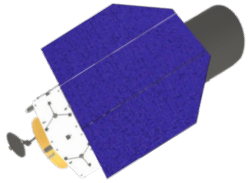

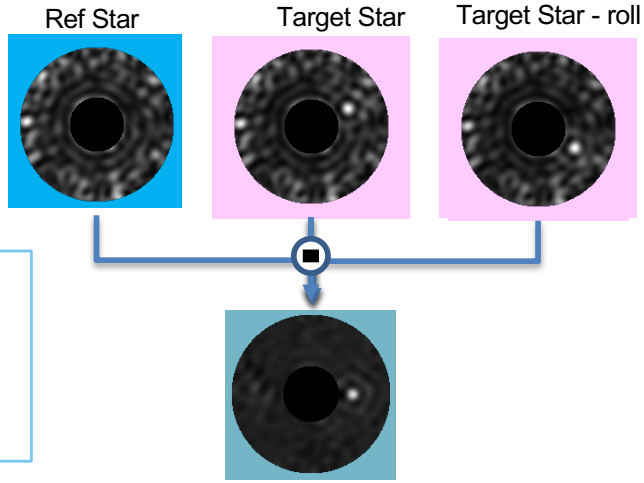

All stars must be **single**
Nothing equally bright within ~45";
increasingly stringent at smaller separations

Target vs Reference should have small delta (spacecraft) pitch for better thermal stability

See also these presentations:
- "Working with Simulated Datasets" (Ygouf)
- "Overview of Observing Scenarios and Their Simulated Datasets" (Krist)
- "Target vetting" (Bailey)

Adapted from J. Krist

Residual tip/tilt jitter impacts contrast, sets V<5 host star requirement

Tip/tilt control on

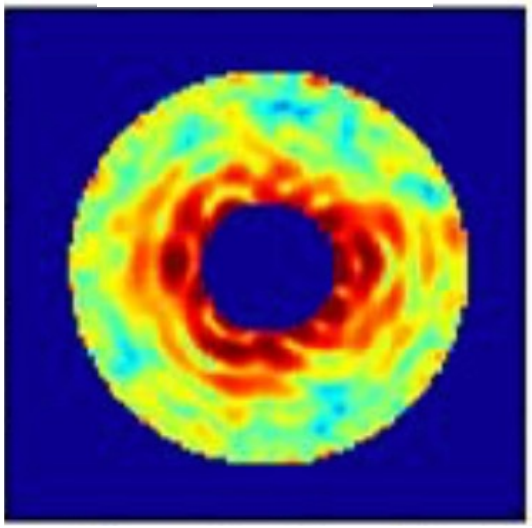

Tip/tilt control off

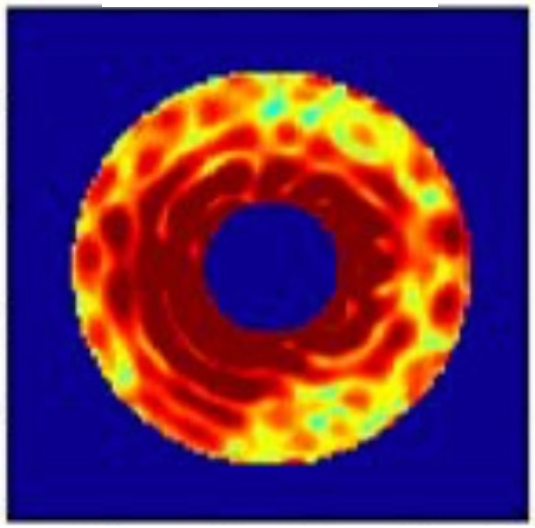

Probably graceful degradation at V>5, but TBD. Project is using V~7 cutoff for coronagraphic target lists. See backup slide about faint star and non-coronagraphic pointing/jitter performance

Shi, F., et al., SPIE, Vol 10698, p 106982O-5 2018 ; flight-like jitter tests on V=5 ”star”
Note: feed-forward will NOT be implemented in flight (ie: tip/tilt control will be feedback only)

Pointing constraints: ±34˚ pitch, ±13˚ roll vs. sun, 22˚ Earth avoidance; 11˚ Moon avoidance

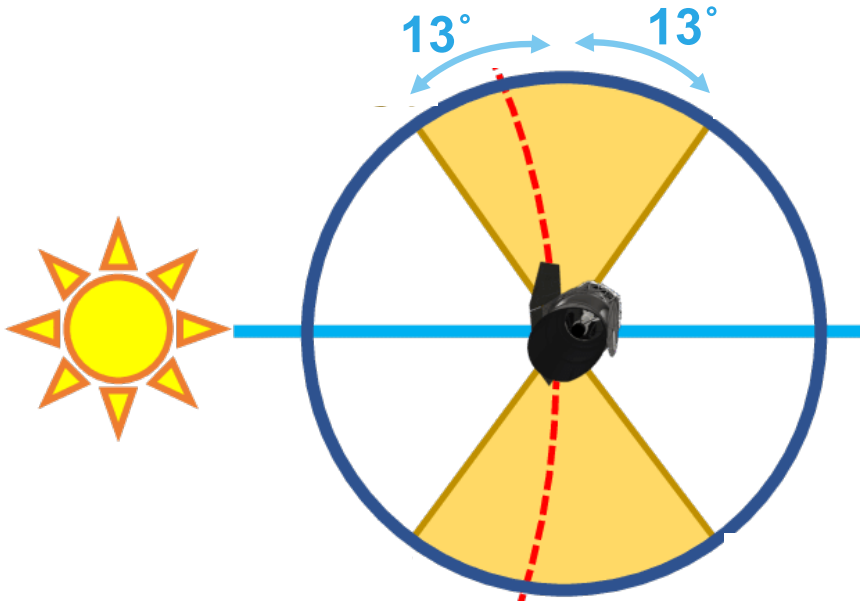

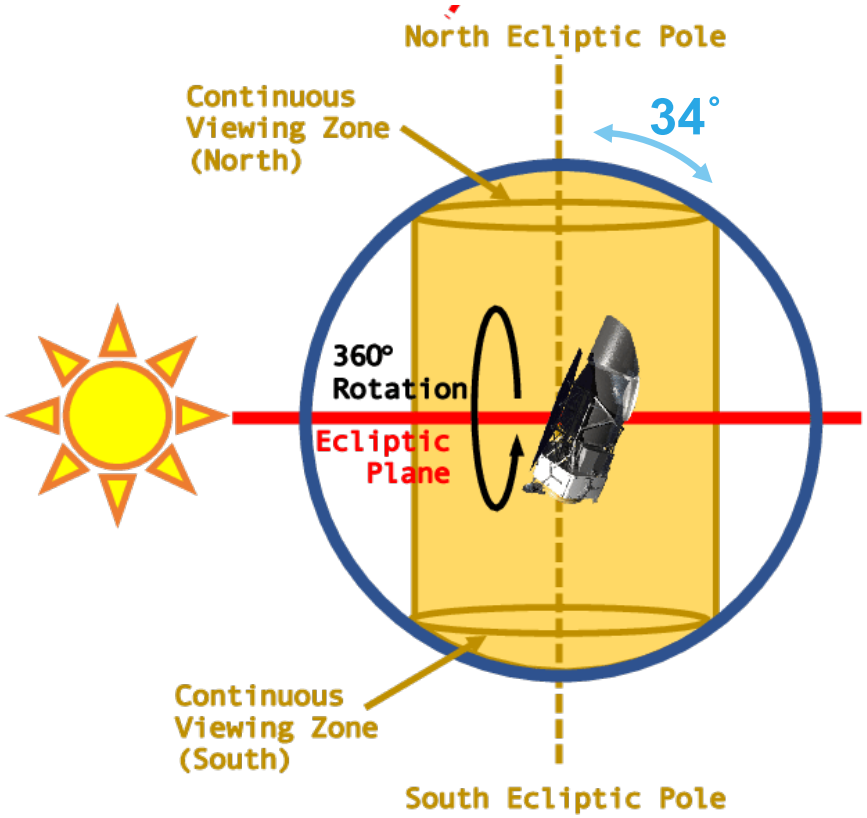

Telescope slew rate for long slews is ~0.05dgr/sec

See Hildebrand Rafels Talk

Hybrid Lyot Coronagraph

- The HLC provides a full 360° high contrast field of view.
- Focal plane occulting mask is a circular, r = 2.8 λ_c/D partially-transmissive nickel disc overlaid with a PMGI dielectric layer with a radially and azimuthally varying thickness profile.
- The HLC design incorporates a numerically optimized, static actuator pattern applied to both deformable mirrors.
- Lyot stop is an annular mask that blocks the telescope pupil edges and struts.

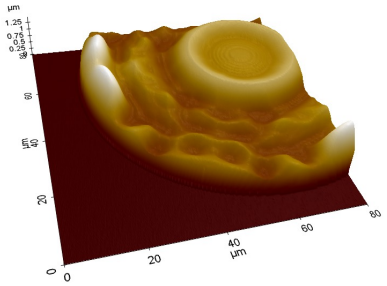

HLC occulting mask. AFM surface height measurement of an occulting mask fabricated by the JPL Micro Devices Lab. Recent design refinements include azimuthal ripples in thickness of the dielectric, which extends across the field of view.

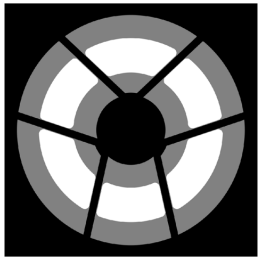

HLC Lyot stop. Diagram of Lyot stop model: white represents the transmitted region; black represents the telescope pupil; gray represents the region blocked by the stop in addition to the telescope pupil.

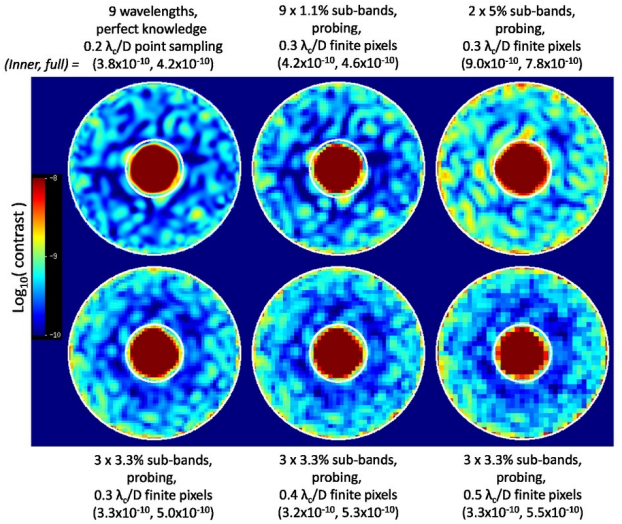

Simulated HLC PSF including aberrations and high-order wavefront control operations, illustrating the annular dark zone between 3 and 9 λ_c/D. Each sub-panel represents a different scenario for DM probe wavelength resolution and detector sampling.

References

- J. Trauger, D. Moody, et al., JATIS Vol 2, id. 011013 (2016) - https://doi.org/10.1117/1.JATIS.2.1.011013
- J. Krist, et al., Proc SPIE Vol 10400, id. 1040004. (2017) - http://dx.doi.org/10.1117/12.2274792
- K. Balasubramanian, et al., Proc SPIE Vol 10400, id. (2017) - https://doi.org/10.1117/12.2274059

Shaped Pupil Coronagraph

- The shaped pupil apodizer is a reflective mask on a silicon substrate with aluminum regions for reflection and black silicon regions for absorption.
- The hard-edged occulting mask has either a bowtie-shaped opening for characterization (spectroscopy) mode or an annular aperture for debris disk imaging.
- The SPC Spectroscopy designed in 2017 produces a 2 x 65° bowtie dark zone from 3.0 – 9.1 λ_C/D over a 15% bandpass.
- The SPC Wide Field of View design produces a 360° dark zone from 5.9 – 20.1 λ_C/D in a 10% bandpass.

Apodizer Mask | Focal Plane Mask | Lyot Stop

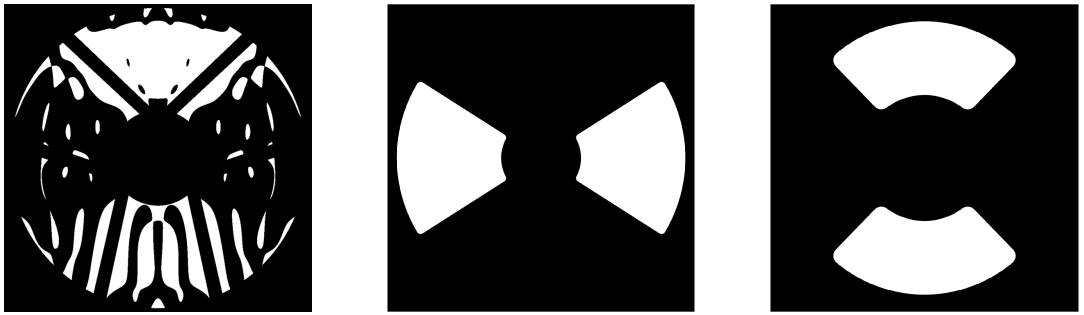

Flight mask designs for the spectroscopy shaped pupil coronagraph.
Design by A.J. E. Riggs (JPL).

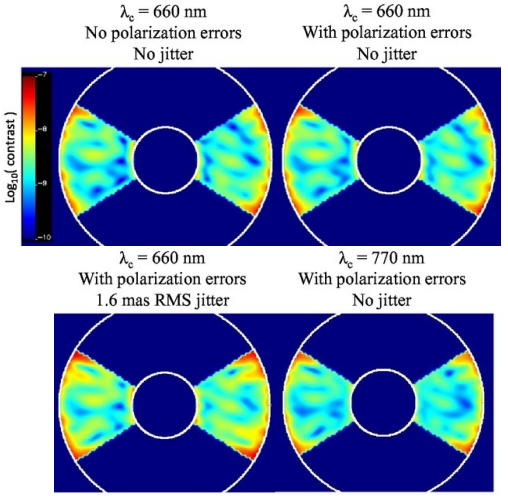

Spectroscopy SPC (2017 design) simulations at λ_C = 660 and 770 nm including system aberrations, pointing jitter, and wavefront control operations. The circles correspond to r = 3 and 9 λ_C/D.

References

- N. T. Zimmerman, et al., JATIS Vol 2 id. 011012 (2016) - http://dx.doi.org/10.1117/1.JATIS.2.1.011012
- K. Balasubramanian, et al., JATIS Vol2 id. 011005 (2015) - https://doi.org/10.1117/1.JATIS.2.1.011005
- A. J. E. Riggs et al., N. T. Zimmerman, et al., Proc SPIE Vol 10400 (2017) - http://dx.doi.org/10.1117/12.2274437
- J. Krist, et al., Proc SPIE Vol 10400, id. 1040004. (2017) - http://dx.doi.org/10.1117/12.2274792

Wavefront Control

- The baseline Roman Coronagraph design includes four active optics to control the wavefront: a **fast steering mirror** (FSM), a flat **focusing mirror** (FCM), and two **deformable mirrors** (DM 1 and DM 2) with 48x48 actuators each.
- High-order wavefront control is implemented by the Electric Field Conjugation (EFC) method. The EFC loop operates on science focal plane data by measuring the interaction of aberrated on-axis starlight with a sequence of DM actuator probes.
- Pointing, focus, and low-order wavefront drifts are sensed by the **Low-Order Wavefront Sensing and Control** (LOWFS/C) subsystem using the Zernike phase-contrast technique on starlight rejected from the occulting mask. Corrections to Zernike modes Z5—Z11 are applied to DM 1.
- The FSM control loop corrects line-of-sight pointing jitter to below 0.95 milliarcsec.

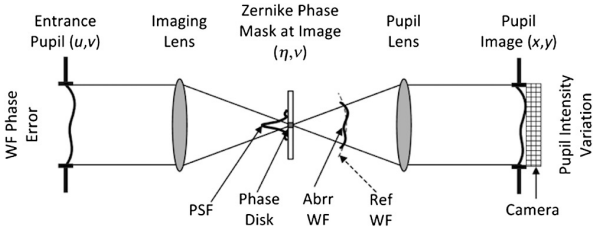

Conceptual diagram of the Zernike phase contrast wavefront sensor (F. Shi, et al., 2016).

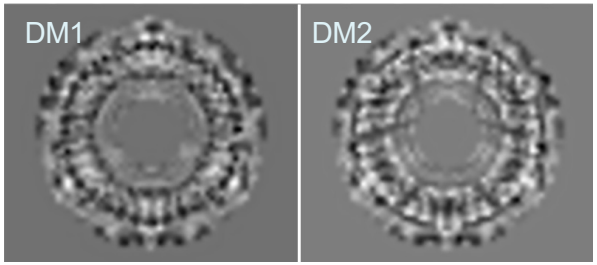

Optimized DM surfaces applied in HLC data simulations.

References

- T. Groff, A. J. E. Riggs, et al., JATIS Vol 2, id 011009 (2015) - https://doi.org/10.1117/1.JATIS.2.1.011009
- F. Shi, et al., JATIS Vol 2, id 011021 (2016) - https://doi.org/10.1117/1.JATIS.2.1.011021
- J. Krist, et al., JATIS Vol 2, id 011003 (2015) - https://doi.org/10.1117/1.JATIS.2.1.011003

Wollaston Prism Polarimetry (Band 1 or 4 imaging)

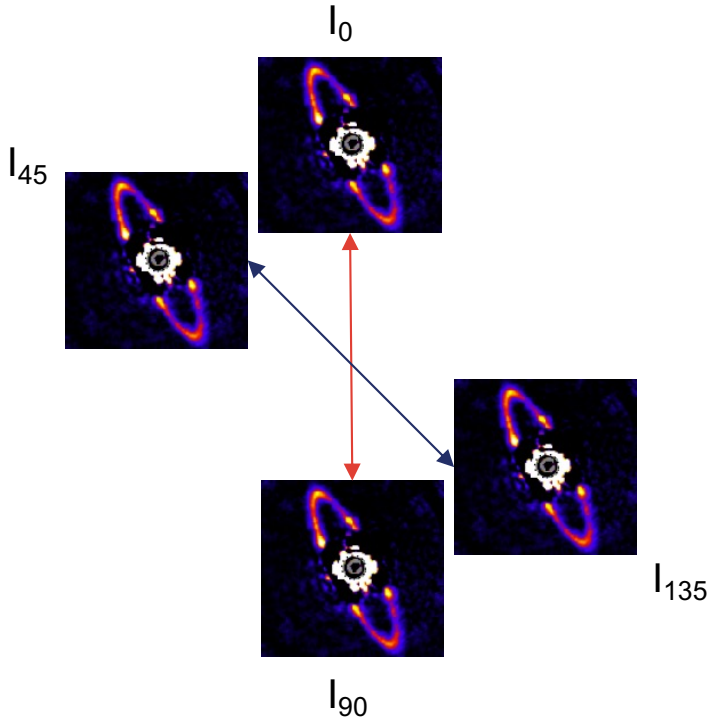

1 pair at a time
Pairs separated by 7.5” on chip

Linear polarized fraction (LPF) goal:
RMSE < 3% *per resel*

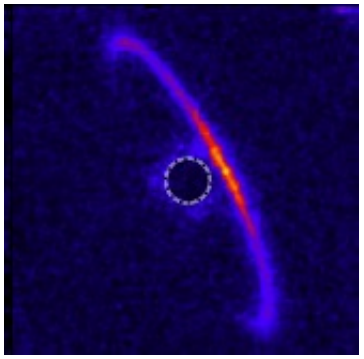

$$LPF = \text{sqrt}\ \{(I_0 - I_{90})^2 + \{(I_{45} - I_{135})^2\}\ /\ I_{tot}$$

R~50 Spectroscopy w/ Slit Spectrograph (Band 3 or 2)

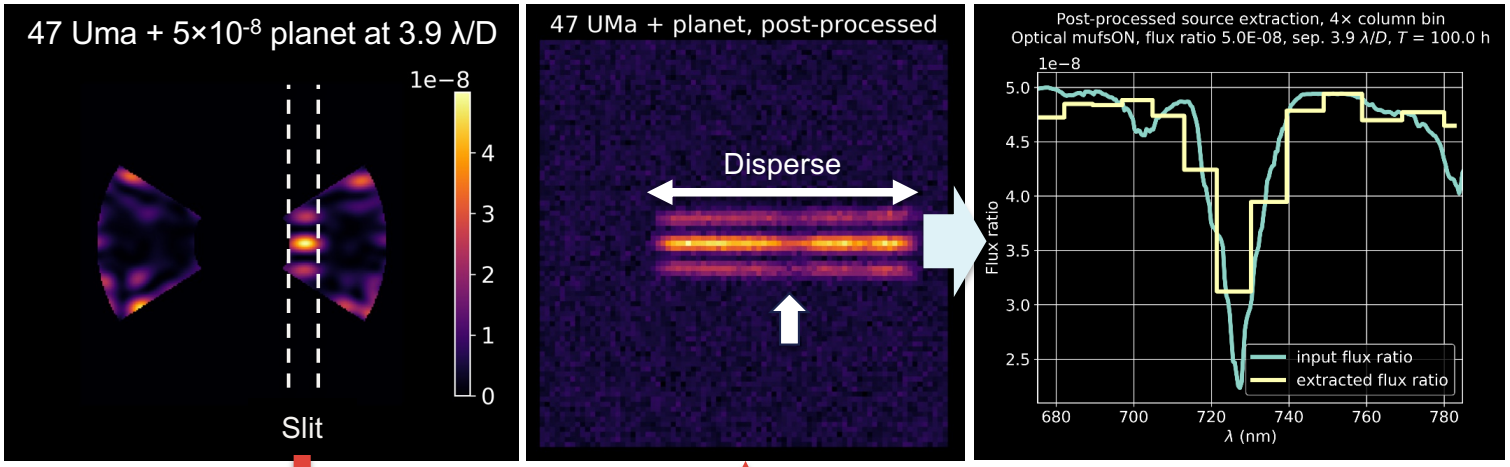

- Slit is deployed to planet position
- Prism disperses the Shaped Pupil PSF
- Spectrum is extracted from image after post-processing (Reference Star Subtraction)
- Variable resolution. R=50 at bandpass center, ±~10

EMCCD Detectors

- Electron Multiplying CCD (EMCCD) technology is advantageous for a coronagraph application.
  - Programmable gain provides wide dynamic range suitable for bright scenes expected during acquisition and coronagraph configuration, while photon counting capability can be used for faint light observations with zero read noise.
- EMCCD detectors are baselined for direct imaging, spectroscopy and wavefront sensing applications in CGI.
  - Subarray readout suitable for a wavefront sensor application enables 1000 frame-s^{-1} operation to accommodate tip-tilt sensing.
- Work at JPL is focused on low flux characterization with radiation damaged sensors.
  - JPL has invested in modifications to the commercial version of the EMCCD that are expected to improve margins against radiation damage in a flight environment.
- JPL's EMCCD test lab has measured a low flux threshold of 0.002 c-psf^{-1}-s^{-1}, equivalent to a 32.4 magnitude star through a 2.4m telescope at 500 nm with 10% bandwidth.
  - Devices irradiated to 5 years equivalent life at L2 meet coronagraph technology requirements.

Radiation-hardened EMCCDs are in Production

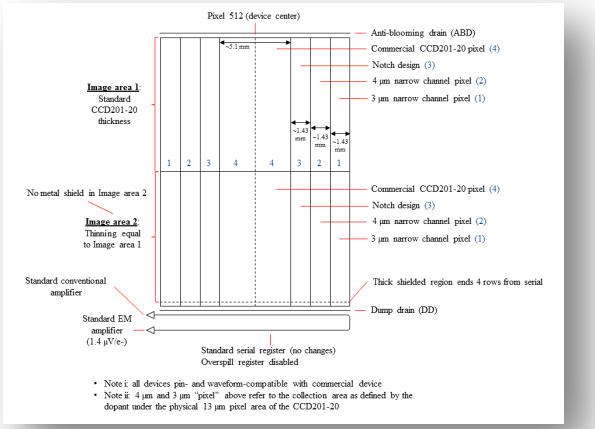

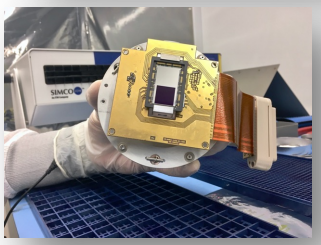

Commercial EMCCD

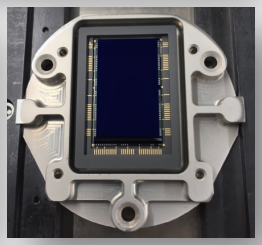

Flight Prototype EMCCD

References

- L. Harding, R. Demers, et al., JATIS Vol 2, id 011007 (2016)

Data Post-processing

- Investigations on algorithms for CGI data post-processing have encompassed both end-to-end data simulations and analysis of laboratory testbed data.
- *Reference differential imaging* (RDI) trials have probed a range of wavefront stability and noise scenarios. Simulations with spacecraft rolls have also enabled tests of *Angular differential imaging* (ADI).

1. Post-Processing of OS9 Simulated HLC-Band 1

From raw to photon-counted data

Classical PSF subtraction

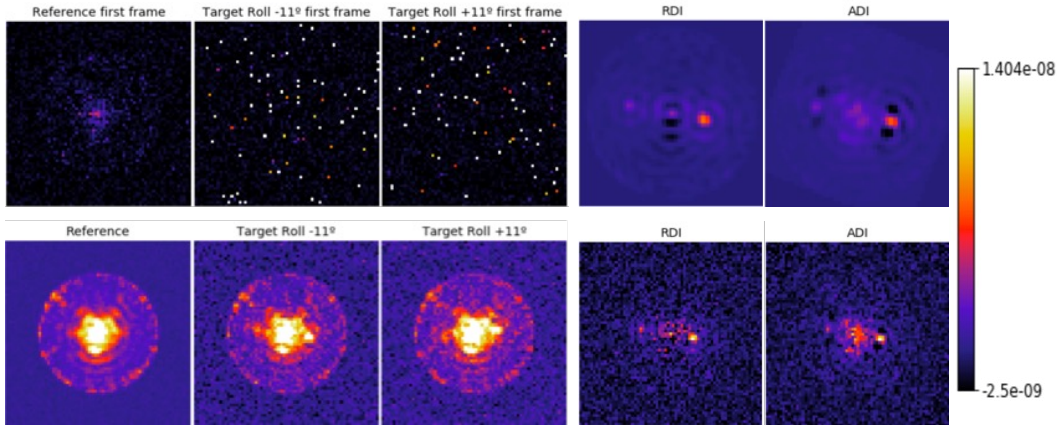

Ygouf et al., 2020

2. Laboratory SPC bow-tie frame recorded at HCIT in a static environment (essentially noiseless other than speckles) with injected fake planet at 10^{-8} flux ratio

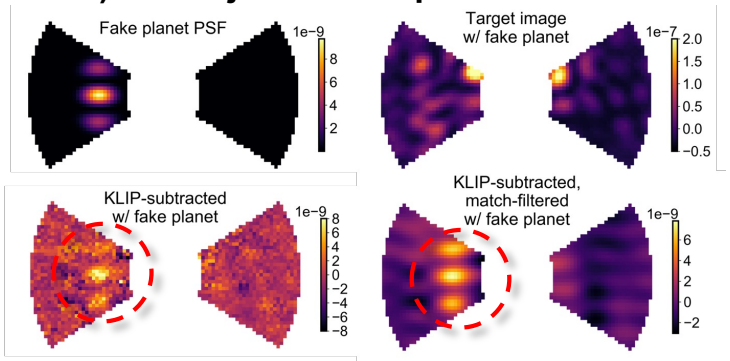

Example application of RDI to SPC data from HCIT, demonstrating the matched-filtered recovery of a fake point source inserted into one image (circled in red)

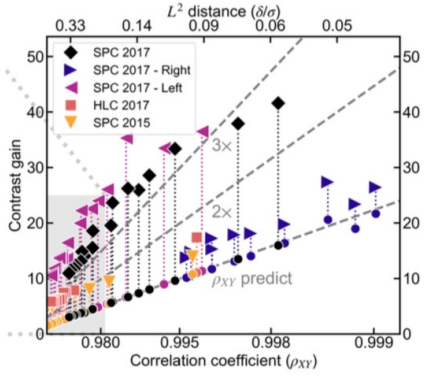

Left: Post-processing contrast gain plotted against reference library correlation for five datasets. Above a certain correlation coefficient, the post-processing gain is comparable to the gain from classical PSF subtraction.

References

- M. Ygouf, N. Zimmerman, L. Pueyo, R. Soummer, et al., Proc. SPIE Vol 9904 (2016) - http://dx.doi.org/10.1117/12.2231581

Ground System Architecture

HOWFS = high-order wavefront sensing
GITL = Ground In The Loop

Data Downlink:
Ka-Band (observation data)
S-Band (commands, housekeeping and HOWFS data)

Raw observation image files ("L1 data products") will be in STScI Archive < 72hr after observation.

CGI scheduling done weeks or months in advance to ensure ground station contact during critical HOWFS GITL periods. CGI does not support 'joysticking' or mid-observation changes!

Purple area of the Observation Data Analysis Environment = "sandbox" area available to CPP and CTC to develop and test data processing algorithms.

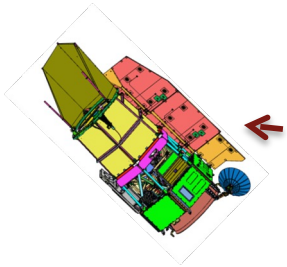

Housekeeping Data and HOWFS GITL Images

Observatory Commands

Mission Operations Center (MOC; GSFC)

Observation Data Files

Observation Planning & Scheduling Products

Science Operations Center (SOC; STScI)

Data Archive

Observation Planning & Data Products

Science Support Center (SSC; IPAC)

Observation Data Analysis Environment

HOWFS Data Analysis Environment

CGI Housekeeping/HOWFS Data

CGI Commands & Products

Coronagraph Community Participation Program (CPP)

Coronagraph Technology Center (CTC; JPL)

Observation Specifications & Data Products

Laboratory Demonstrations

Results from the Occulting Mask Coronagraph (OMC) Testbed at JPL HCIT

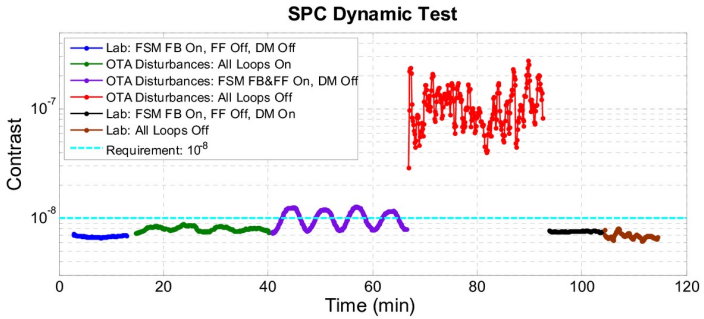

Dynamic contrast demonstration with a Low Order Wavefront Sensing and Control (LOWFS/C) system integrated on the Occulting Mask Coronagraph testbed. When line-of-sight disturbances and low order wavefront drift (slow varying focus) are introduced on the testbed, the LOWFS senses the pointing error and wavefront drift and corrects them by commanding a fast steering mirror and one of the DMs. Demonstrations with both the SPC and HLC masks surpassed their 1E-8 contrast goal (F. Shi, et al., Proc SPIE Vol 10400, 2017).

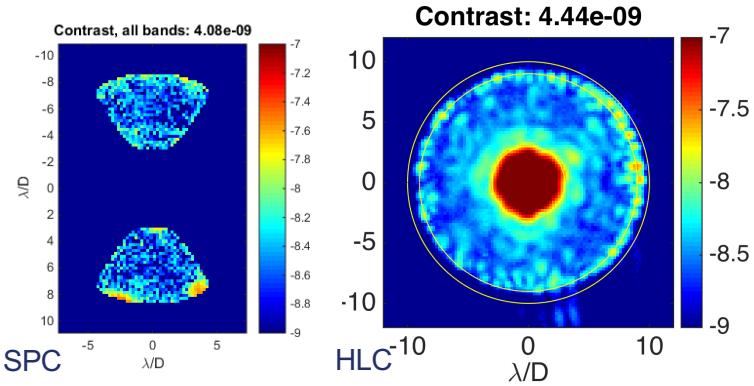

Normalized intensity maps measured on the OMC testbed in broadband (10 %) light for SPC (left) and HLC. The total contrast between 3 – 9 λ/D is listed on top of each figure.

References

- F. Shi, E. Cady, et al., Proc. SPIE Vol 10400 (2017) - http://dx.doi.org/10.1117/12.2274887
- E. Cady, K. Balasubramanian, et al., Proc. SPIE Vol 10400 (2017) - http://dx.doi.org/10.1117/12.2272834
- B.-J. Seo, E. Cady, et al., Proc SPIE Vol 10400, 10.1117/12.2274687 (2017) - http://dx.doi.org/10.1117/12.2274687
- F. Shi, et al., Proc. SPIE Vol 10698 (2018) - https://doi.org/10.1117/12.2312746
- B.-J. Seo, et al, Proc. SPIE Vol 10698 (2018) - https://doi.org/10.1117/12.2314358
- D. Marx, et al, Proc. SPIE Vol 10698 (2018) - https://doi.org/10.1117/12.2312602
- F. Shi, et al., Proc. SPIE Vol 11117 (2019) - https://doi.org/10.1117/12.2530486

Simulations Resources

Name	Author	Description	Format	URL	References
WFIRST Coronagraph Instrument (CGI) Imaging Simulations	John Krist (JPL)	Time series CGI imaging data simulations produced by JPL, incorporating observatory STOP models and wavefront control.	FITS files	https://roman.ipac.caltech.edu/sims/Coronagraph_public_images.html	J. Krist, et al., JATIS Vol 2, id. 011003 (2016) J. Krist, et al., Proc SPIE Vol 10400, id. 1040004. (2017)
EXOSIMS	Dmitry Savransky (Cornell U.)	Exoplanet Open-Source Imaging Mission Simulator, with dedicated configurations for simulating CGI surveys and integration times.	web browser interface	https://roman.ipac.caltech.edu/sims/tools/exosimsCGI/exosimsCGI.html	D. Savransky & D. Garrett, JATIS Vol 2, id. 011006 (2016) C. Delacroix, D. Savransky, et al., Proc SPIE Vol 9911, id. 991119 (2016)
			Python source code	https://github.com/dsavransky/EXOSIMS	
WebbPSF	Marshall Perrin (STScI)	Simulated Point Spread Functions for WFIRST WFI and CGI (static)	Python source code, with tutorials	https://github.com/mperrin/webbpsf	M. Perrin, et al., Proc SPIE Vol 8442, article id. 84423D (2012) M. Perrin, et al., Proc SPIE Vol 9143, id. 91433X (2014)

Simulations Resources

Name	Author	Description	Format	URL
Fast Linearized Coronagraph Optimizer (FALCO)	AJ Riggs (JPL)	wavefront correction simulator, DM-integrated coronagraph design, testbed operation. CGI simulations	MATLAB and Python3 source codes with Wiki	https://github.com/ajeldorado/falco-matlab https://github.com/ajeldorado/falco-python https://github.com/ajeldorado/falco-matlab/wiki
FALCO + WFIRST CGI PROPER model	AJ Riggs (JPL)	Run end-to-end HOWFSC with the official Phase B model of the WFIRST CGI; Produces: CGI dark hole images and performance tables	MATLAB	https://github.com/ajeldorado/falco-matlab/wiki/01b%29-Examples-using-the-WFIRST-CGI-PROPER-model

Reference Documents

Caveat: performance predictions have degraded over time; you should sanity check older papers' conclusions against the latest contrast curves!

Reference	URL	Year
Wide-Field Infrared Survey Telescope-Astrophysics Focused Telescope Assets (WFIRST-AFTA) 2015 Report by the Science Definition Team (SDT) and WFIRST Study Office	https://roman.gsfc.nasa.gov/science/sdt_public/WFIRST-AFTA_SDT_Report_150310_Final.pdf	2015
Journal of Astronomical Telescopes Instruments and Systems, Vol. 2, No. 1, Special Section on WFIRST-AFTA Coronagraphs, eds. Olivier Guyon and Motohide Tamura	https://www.spiedigitallibrary.org/journals/Journal-of-Astronomical-Telescopes-Instruments-and-Systems/volume-2/issue-01#Editorial	2016
SPIE Proceedings Vol. 10400, Techniques and Instrumentation for Detection of Exoplanets VIII, ed. Stuart Shaklan	https://www.spiedigitallibrary.org/conference-proceedings-of-spie/10400	2017
SPIE Proceedings Vol. 10698, Space Telescopes and Instrumentation 2018: Optical, Infrared, and Millimeter Wave, WFIRST I, II, III	https://www.spiedigitallibrary.org/conference-proceedings-of-spie/10698	2018
Community White Papers submitted to the NAS Exoplanet Science Strategy Committee, co-chairs D. Charbonneau & S. Gaudi. Among the CGI-related papers are: Kasdin et al., Bailey et al., Mennesson et al., Marley et al., B. Crill et al., and others.	http://sites.nationalacademies.org/SSB/CurrentProjects/SSB_180659	2018
The Wide Field Infrared Survey Telescope: 100 Hubbles for the 2020s, Akeson et al., 2019, Astro2020 white papers	https://arxiv.org/pdf/1902.05569.pdf	2019

Reference Documents

Caveat: performance predictions have degraded over time; you should sanity check older papers' conclusions against the latest contrast curves!

Reference	URL	Year
SPIE proceedings: 2018 Vol 10698; 2019 Vol 11117; 2020 Vol 11443; 2021 Vol 11823	https://spie.org/publications/conference-proceedings	2018-2022
Absolute Flux Calibrations for the Nancy Grace Roman Space Telescope Coronagraph Instrument	https://ui.adsabs.harvard.edu/abs/2022arXiv220703607P/abstract	2022
Flatfield Calibrations with Astrophysical Sources for the Nancy Grace Roman Space Telescope's Coronagraph Instrument	https://ui.adsabs.harvard.edu/abs/2022arXiv220204815M/abstract	2022
Nancy Grace Roman Space Telescope Coronagraph Instrument Observation Calibration Plan	https://ui.adsabs.harvard.edu/abs/2022arXiv220205923Z/abstract	2022

Web Resources

- JPL Roman Coronagraph Website
  - https://www.jpl.nasa.gov/missions/the-nancy-grace-roman-space-telescope/
  - Coronagraph Overview and Capability
- Goddard Roman Website
  - https://roman.gsfc.nasa.gov
  - Mission Overview
  - Science Overview
  - Resources (images and multimedia, documents, newsroom, and press releases)
- Roman at IPAC
  - https://roman.ipac.caltech.edu
  - Science Overview
  - Documentation
  - Simulations (both WFI and the Coronagraph)
  - Community Engagement (including Workshops, Meetings and Talks and Preparatory Science)
    - Roman Virtual Lecture Series https://roman.ipac.caltech.edu/Lectures.html
  - Publications